Dual-scale modeling of proton-exchange membrane fuel cell for degradation assessment

QiAn He[1], Zhongliang Li[1], Nadia Yousfi Steiner[1], Daniel Hissel[1,2]

[1]Université Marie et Louis Pasteur, UTBM, CNRS, institut FEMTO-ST, FCLAB, F-90000 Belfort, France
[2]Institut Universitaire de France (IUF), France

Abstract : Hydrogen is known as one of the cleanest energy carriers. To meet the challenge of applying hydrogen energy to transportation in a reliable way, continuous health monitoring and assessment of fuel cell systems are essential to the long-term daily operation and maintenance schedule. In this context, this paper presents a brief literature review of the modeling methods dedicated to the health management of proton exchange membrane fuel cells and reports a dual-scale degradation modeling method developed in a Python environment. The potential of this modeling tool for long-term degradation assessment and health index identification has been justified through several case studies.

Key words - PEMFC, Catalyst layer, Degradation, Modeling, Health management

1. INTRODUCTION

Due to the advantage of high efficiency and low-carbon emission, proton-exchange membrane fuel cell (PEMFC) has been one of the promising technologies with the potential to address the global challenge of energy resources and climate change. However, the unsatisfactory lifespan and cost are still the major concerns affecting the wide commercial utilization of PEMFC in transportation and power systems. Under these circumstances, numerous recent academic publications have been focused on the study of the PEMFC degradation behaviors in various applications, such as microgrids and transportation [1, 2, 3]. The cell voltage and power are commonly utilized as the health indicator during a steady-state operation, meanwhile, electrochemical surface area (ECSA) and resistance are focused for health identification during dynamic operation [2]. Currently, most of the existing literature on PEMFC degradation assessment is predominantly dedicated to determining the pattern of voltage decay rates corresponding to some ideal load condition [4]. The majority of methods applied to this topic include model-based and learning-based methods. It's worth noticing that, along with the development of artificial intelligence, physics-based modeling techniques tend to play an increasingly important role within learning-based methods to enhance their interpretability and generalization. To address the challenge of developing multiple health indicators for PEMFC degradation assessment, this study investigates a physical model of the degradation of platinum (Pt) catalyst particles. More importantly, the proposed model is integrated in a dual-scale modeling framework enabling the linkage between macro-scale operation and micro-scale material degradation. In case studies, the degradation behaviors under different operating conditions are simulated using the proposed model. Thus, the understanding of catalyst degradation impact factors is strengthened. Finally, the potential of the proposed model in health-enhancement control and preventive maintenance of PEMFC systems is discussed.

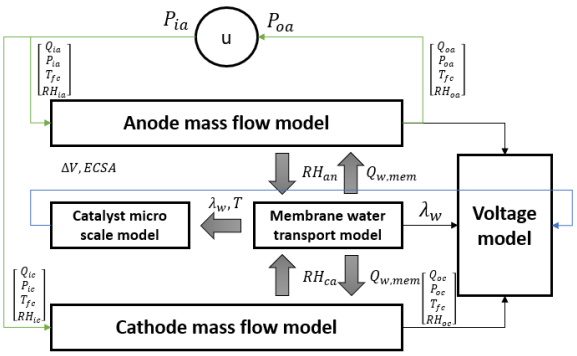

FIG. 1. The structure of the Python-based PEMFC simulation model

2. PEMFC DEGRADATION MODELING

In order to track the degradation of voltage and catalyst layer (CL), we report a modeling method that involves a multiphysics dynamic model associated with a catalyst degradation model. The parameters such as voltage, flow rate, and water content of the membrane can be tracked from the former, meanwhile, micro-scale conditions such as the distribution of the platinum radius distribution can be evaluated based on the latter. Different behaviors tend to be observed on this dual-scale model by applying several long-term dynamic load profiles so that the degradation can be evaluated by simulating this model which is realized in Python.

2.1. PEMFC degradation modeling - micro-scale model

The catalyst of PEMFC, which is mainly composed of platinum particles deposed on carbon base, is devoted to enhancing the oxygen-reduction reaction (ORR) on the cathode side and hydrogen evolution reaction (HER) on the anode side. The mechanism of catalyst degradation has been explored for decades. Regarding the platinum particles, the degradation is mainly attributed to dissolution and oxidation, and in this context they struggle to maintain the structure, thereby compromising the optimal performance of PEMFC. Regarding the carbon support the corrosion mechanism is typical cause. In our model, platinum dissolution, re-deposition, oxidation, and carbon detachment are involved, as described by the following equations respectively :

$$Pt \leftrightarrow Pt^{2+} + 2e^- \tag{1}$$

$$Pt + H_2O \leftrightarrow Pt - O + 2H^+ + 2e^- \tag{2}$$

$$Pt - O + 2H^+ \leftrightarrow Pt^{2+} + H_2O \tag{3}$$

$$C + 2H_2O \rightarrow CO_2 + 4H^+ + 4e^- \tag{4}$$

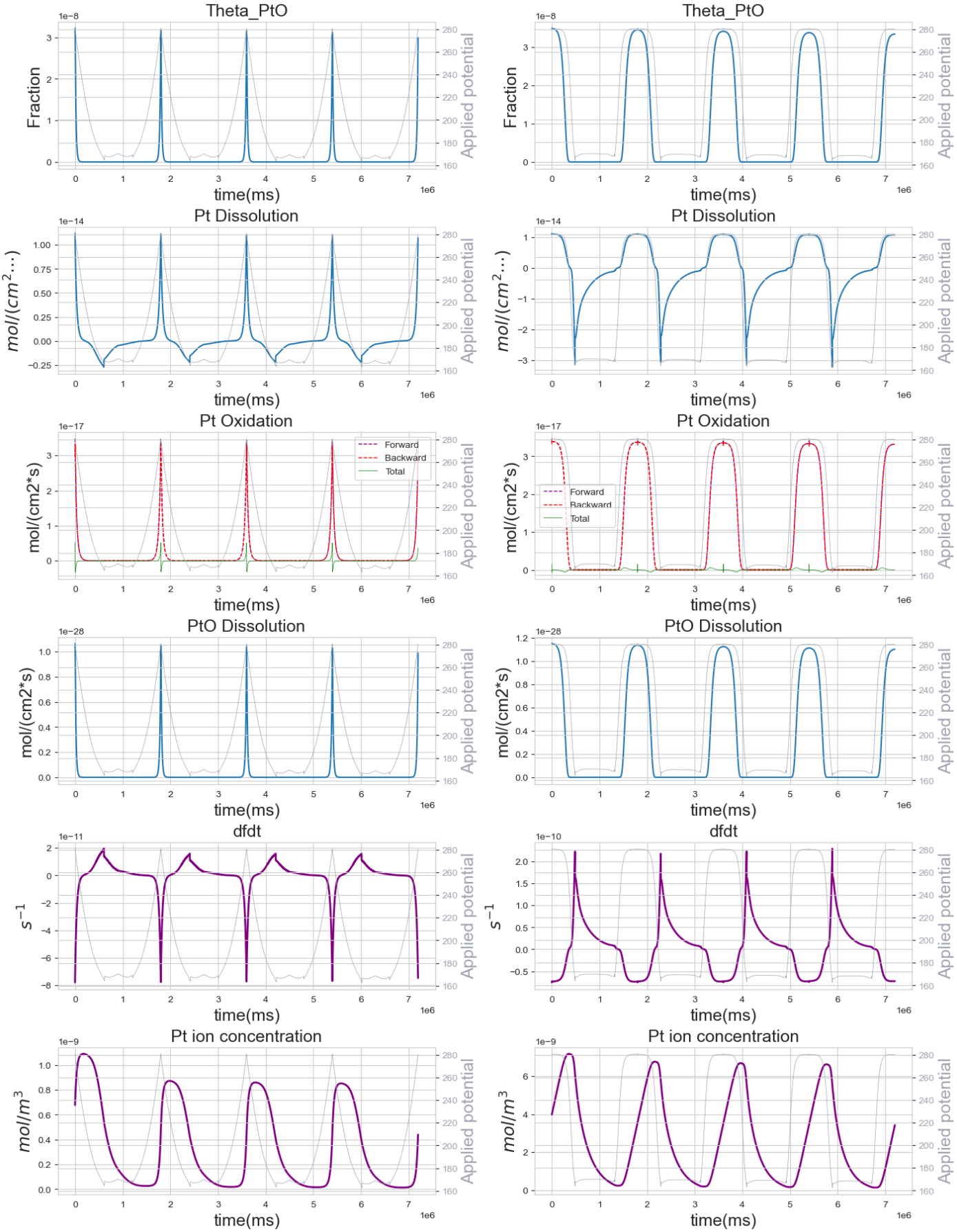

FIG. 2. The kinetic of catalyst degradation in terms of the triangle load profile(left) and rectangle load profile(right).

The modified Butler-Volmer models quantifying the kinetics of the dissolution and oxidation reactions are given as [5] :

$$r_1 = k_1[(1-\theta_{PtO})\exp\left(\frac{\alpha_{a,1}n_1F}{RT}(U-U_1^{eq})\right) - \left(\frac{c_{\mathrm{Pt^{2+}}}}{c_{\mathrm{Pt^{2+},ref}}}\right)\exp\left(-\frac{\alpha_{c,1}n_1F}{RT}(U-U_1^{eq})\right)] \tag{5}$$

$$r_2 = k_2[exp\left(\frac{\omega\theta_{PtO}}{RT}\right)\exp\left(\frac{\alpha_{a,2}n_2F}{RT}(U-U_2^{eq})\right) -\theta_{PtO}\left(\frac{c_{\mathrm{H^+}}}{c_{\mathrm{H^+,ref}}}\right)\exp\left(-\frac{\alpha_{c,2}n_2F}{RT}(U-U_2^{eq})\right)] \tag{6}$$

The chemical dissolution rate [7] :

$$r_3 = k_3\theta_{PtO}c_{H^+}^2 \tag{7}$$

And the rate of carbon detachment [7] :

$$r_4 = k_{det}\frac{M_c}{\rho_c}exp(\frac{\alpha_{det}F}{RT}(U-U_4^{eq}))\frac{1}{r} \tag{8}$$

The concentration-dependent expression built the relationship between the controlled pressure of the inlet gas with the degradation kinetic. The evolution of the platinum ion is[5] :

$$\frac{dc_{Pt^{2+}}}{dt} = -\frac{m_v}{M_{Pt}}(\frac{4\pi\rho_{Pt}\int_0^\infty r^2 f_N(r,t)(\frac{dr}{dt}-r_3)dr}{\frac{4}{3}\pi\rho_{Pt}\int_0^\infty r^3 f_N(r,0)dr}) \tag{9}$$

Here $m_v = 1e-3$, $M_{Pt} = 195.1g/mol)$, and $\rho_{Pt} = 21.45g/cm^3$ denotes the mass loading of platinum per volume, the platinum molar mass, and the density of platinum. In this equation, we neglect the mechanism of platinum loss to the membrane. By carrying out the simulated accelerating stress test (AST) where the fuel cell operation under long-term triangle and rectangle load profile, the current of which ranged from 20A to 110A, the particle radius distribution (PRD) demonstrates a prominent shift with respect to time, which is described in the form of partial differential equation (PDE) [7] :

$$\frac{\partial f_N(r,t)}{\partial t} = -\frac{\partial}{\partial r}\left[f_N(r,t)\frac{dr}{dt}\right] + J^+ - J^- - R_4(r,t)f_N(r,t) \tag{10}$$

where $f_N(r,t)$, r, J^+, J^-, R_4 refers to the particle radius distribution, the particle creation and extinction of the coagulation process, and the detachment degradation mechanism on the carbon cloth. To improve the execution time, we neglect J^+ and J^- because their value is on an order of magnitude smaller than the other terms [13]. That is, in this case, the developed model takes advantage of the Ostwald ripening, dissolution, oxidation, and carbon detachment mechanism to access the CL degradation, the simplification is given as :

$$\frac{\partial f_N(r,t)}{\partial t} = -\frac{\partial}{\partial r}\left[f_N(r,t)\frac{dr}{dt}\right] - r_4 f_N(r,t) \tag{11}$$

The initial distribution is subject to, for instance, a log-normal distribution :

$$f_N(ln(r),0) \sim \mathcal{N}(\mu,\sigma^2) \tag{12}$$

where μ and σ denote the mean and standard deviation of the PRD according to experimental data. The change rate of the radius of each group of particles is given as :

$$\frac{dr}{dt} = V_m k_{rdp} c_{Pt} e^{-\frac{R_0}{r}} - V_m(r_1+r_2)c_{Pt}e^{-\frac{R_0}{r}} \tag{13}$$

where k_{rdp} denotes the Ostwald ripening rate, the experimental result of which can be found in [5]. $V_m = 9.9cm^3/mol$ denotes the molar volume of platinum. R_0 denotes the characteristic radius as given :

$$R_0 = \frac{V_m\gamma_{Pt}}{RT} \tag{14}$$

$\gamma_{Pt} = 2.37e-4J/cm^2$ denotes the surface tension of platinum. Hence, the total surface area of the platinum particle can be obtained from the spatial integral of PRD [7], as

$$S(t) = 4\pi\int_{r_{min}}^{r_{max}} r^2 f_N(r,t)dr \tag{15}$$

The normalized ECSA is utilized as one of the health indicators :

$$S_N(t) = \frac{4\pi\int_{r_{min}}^{r_{max}} r^2 f_N(r,t)dr}{4\pi\int_{r_{min}}^{r_{max}} r^2 f_N(r,0)dr} \tag{16}$$

On the other hand, the PtO coverage that formed from the dissolved Pt ions is expressed as :

$$\frac{d\theta}{dt} = \frac{r_2-r_3}{\Gamma_{max}} - \frac{2\theta}{r}\frac{dr}{dt} \tag{17}$$

Here Γ_{max} denotes the mole number of the active sites per unit of per platinum area. The effective ECSA impacts the exchange current density consequently [**?**] :

$$i_0 = i_0^{ref}S_N(t)\left(\frac{P_{O_2}}{P_{ref}}\right)^\gamma \cdot exp\left[\frac{G_{red}}{RT}(1-\frac{T}{T_{ref}})\right]exp\left(-\frac{\omega\theta}{RT}\right) \tag{18}$$

G_{red} denotes the activation energy for O_2 reduction on platinum particles. The membrane degradation mainly accounts for the membrane thickness evolution, as a result of the release of fluorine in the Nafion membrane, as given by [6] :

$$\frac{d\delta_{mb}}{dt} = k_m\psi_{O_2}\frac{P_{O_2}}{\delta_{mb}}exp(\frac{\alpha_m F}{RT}U(t))exp(\frac{E_m}{R}(\frac{1}{T}-\frac{1}{T_0})) \tag{19}$$

k_m, α_m and E_m denote the equivalent fluoride released rate, transfer coefficient, and the equivalent activation energy which can be found in the fitting result of experimental value [13].

2.2. PEMFC degradation modeling - macro-scale model

The macro-scale model is dedicated to simulating the real-time system dynamics under different control commands and operation conditions. The structure of the coupled two models is demonstrated in Figure 2. In the macro-scale model, the voltage is calculated as

$$V_{FC} = E_o - E_{ohm} - E_{act} - E_{con} \tag{20}$$

E_{ohm},E_{act}, and E_{con} denote the ohmic loss, the activation loss and the concentration loss separately, While the open circuit voltage is given based on Nernst equation [7] :

$$E_0 = 1.229 - 8.5*10^{-4}(T_{FC}-298.15) + \frac{RT}{4F}ln(P_{H_2}P_{O_2}^{1/2}) \tag{21}$$

The ohmic loss, activation loss, and concentration loss are presented as :

$$E_{ohm} = i(R_{ohm}+r_{ohm}t) \tag{22}$$

$$E_{act} = \frac{RT}{\alpha F}ln(\frac{i}{i_0}) \tag{23}$$

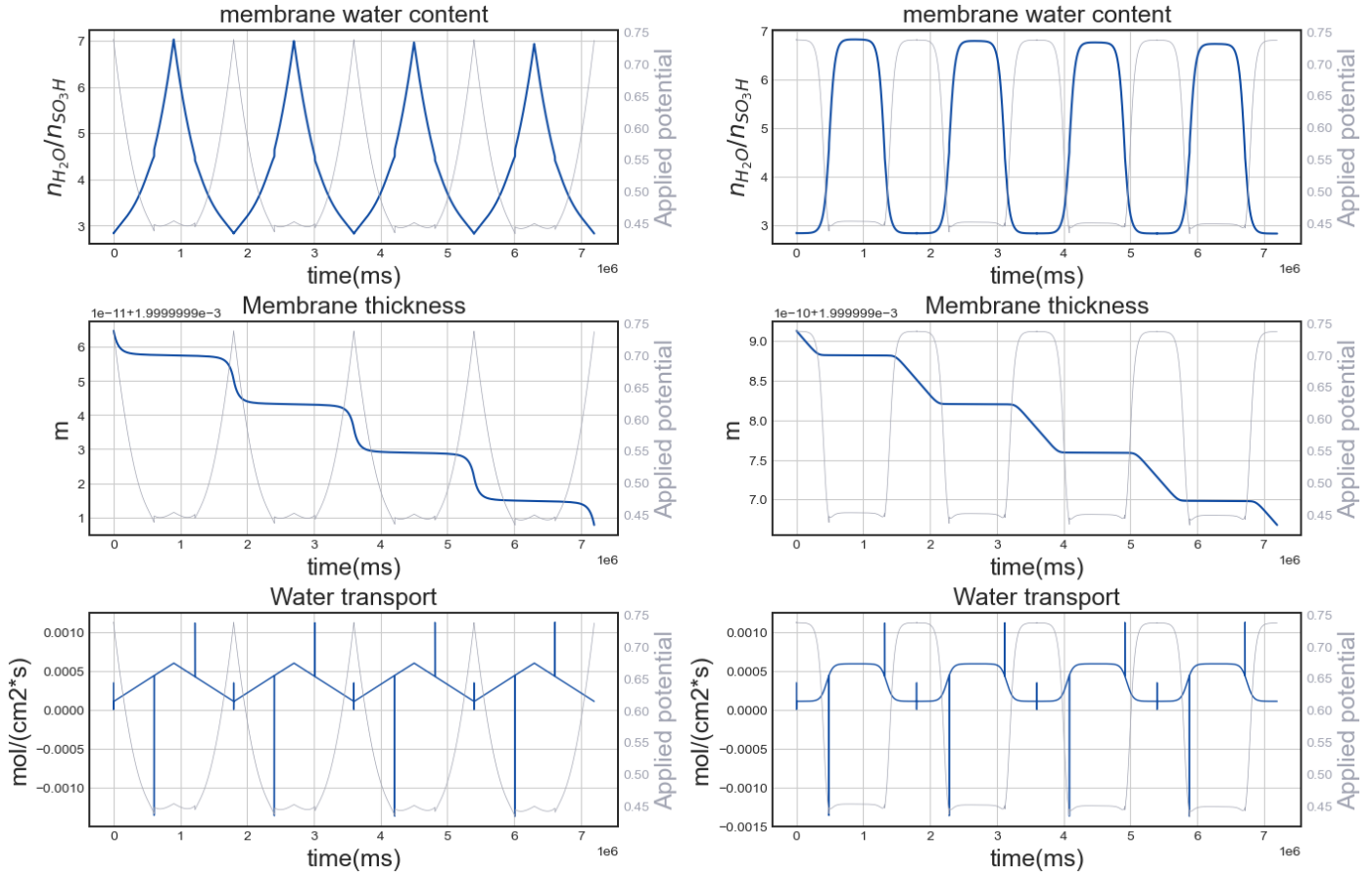

FIG. 3. The evolution of the membrane thickness under triangle load profile

$$E_{con} = R_{O_2} i_{max}^{ref} \tag{24}$$

R, T, and F refer to the universal gas constant, fuel cell temperature, and Faraday constant. r_{ohm} refers to the fitted deviation coefficient representing the increased ohmic resistance with time. The constants are given in the table below and the operation temperature is 80 degrees in this case. i_0 denotes the aforementioned exchange current density. Combining the spatial-uniform flow channel model proposed in [11], a state equation was established to model the change of the internal mass state of the PEMFC while incorporating the control input :

$$\begin{bmatrix} \frac{dM_{H_2,\text{an}}}{dt} \\ \frac{dM_{w,\text{an}}}{dt} \\ \frac{dM_{O_2,\text{ca}}}{dt} \\ \frac{dM_{N_2,\text{ca}}}{dt} \\ \frac{dM_{vp,\text{ca}}}{dt} \end{bmatrix} = \begin{bmatrix} Q_{ia,H_2} - Q_{oa,H_2} - Q_{r,H_2} \\ Q_{ia,vp} - Q_{oa,vp} - Q_{m,vp} - Q_{oa,l} \\ Q_{ic,O_2} - Q_{oc,O_2} - Q_{r,O_2} \\ Q_{ic,N_2} - Q_{oc,N_2} \\ Q_{ic,vp} + Q_{\text{cgen},vp} + Q_{m,vp} - Q_{oc,vp} - Q_{oc,l} \end{bmatrix} \tag{25}$$

where Q and M denote the flow rate (g/s) and weight (g). The subscripts i and o refer to the inlet and outlet, corresponding to the cathode and anode which are represented by the c and a respectively. vp and l denote the vapor and liquid water flow respectively. It is clear that in these equations, the derivatives of the mass weights of hydrogen, oxygen, nitrogen, and water are directly linked to the inlet, outlet, chemical reaction, and membrane mass flow. The mass flow of each kind of gas can be derived from the control input based on ideal gas law, relative humidification, and the vapor saturation pressure regression value. The flow rates of hydrogen and oxygen that participate in chemical reactions remain constant if the load current doesn't change.

In this model, the mass flow of the anode Q_{ia} is controlled by the feedback from the anode outlet by a proportional controller, as a result, to maintain the pressure of the anode[11]. While the cathode inlet mass flow is assumed to remain unchanged thus the supply manifold pressure on the cathode side $p_{csm} = 1.5bar$ is used as the set point. On the anode side, the outlet pressure is used as the feedback signal as we assume that the manifold volume is lumped with the anode volume. That is :

$$p_{out,an} = p_{H_2,an} + p_{v,an} \tag{26}$$

The pressure of each term can be obtained from the ideal gas law :

$$p_{H_2,an} = \frac{m_{H_2,an} R_{H_2} T_{fc}}{V_{an}} \tag{27}$$

$$p_{v,an} = \frac{m_{v,an} R_v T_{fc}}{V_{an}} \tag{28}$$

The controller model is given as :

$$Q_{ia} = K_1(K_2 p_{csm} - p_{out,an}) \tag{29}$$

The objective of this design is to minimize the pressure across the membrane between the cathode and the anode. Two empirical parameters $K_1 = 1e3(\frac{g/s}{kPa})$ and $K_2 = 9e-4$ were defined based on the performance of the controller, by which the anode pressure presented a good tracking to the cathode pressure.

3. CASE STUDY

The proposed dual-scale degradation model is implemented in a Python environment. At each time step of computation, the aforementioned internal conditions are calculated at a fixed time step. The initial value of the mass of each species is given as in the table 3. Figure 4 presents the solution at a fixed time step

TABLEAU 1. Constant table

Symbol	Description	Value	Unit
k_1	Reaction rate constant of Pt dissolution	3e-9[5]	$mol/(cm^2 \cdot s \cdot K)$
$k_{1,ref}$	Referece reaction rate constant of Pt dissolution	1e-18[5]	$mol/(cm^2 \cdot s \cdot K)$
k_2	Reaction rate constant of Pt oxidation	1e-13[5]	$mol/(cm^2 \cdot s \cdot K)$
$k_{1,ref}$	Referece reaction rate constant of Pt oxidation	1e-13[5]	$mol/(cm^2 \cdot s \cdot K)$
k_3	Reaction rate constant of Pt oxide dissolution	1e-15[5]	$mol/(cm^2 \cdot s \cdot K)$
k_{det}	Reaction rate constant of carbon detachment	1.8e-22	$mol/(cm^2 \cdot s \cdot K)$
k_{rdp}	Reaction rate constant of redeposition	1e-10[5]	$mol/(cm^2 \cdot s \cdot K)$
R	Universal gas constant	$J.mol^{-1}.K^{-1}$	8.314
F	Faraday constant	$C.mol^{-1}$	96485

TABLEAU 2. Simulation setup & operation condition

Operation condition	Value
Temperature(K)	353
Number of cells	381
Maximum load current(A)	110
Minimum load current(A)	55
Maximum Pt particle radius (cm)	1e-6
Minimum Pt particle radius (cm)	1e-8
Initial membrane thickness (m)	2e-5
Load profile	Triangle&rectangle
Duration	1 hour
Set point of anode inlet pressure	1.4bar

TABLEAU 3. Initial values for numerical solution

$m_{H_2,an}$	$m_{H_2O,an}$	$m_{O_2,ca}$	$m_{H_2O,ca}$	$m_{N_2,ca}$
0.00033	0.0013	0.0012	0.386	0.0078

and set point controlling. The simulation file was executed on a workstation equipped with an i7-11850H CPU. The main objective of this study is to evaluate and explain the degradations under different dynamic load profiles. The microscale model is developed to evaluate the catalyst degradation that leads to the loss of activation area across different load profiles. So that the deduced voltage drop can be predicted in advance for further management objectives. To implement the microscale model, the reaction constants which are given in Table I were utilized. They were obtained based on the previous literature that conducted AST for the fuel cell system under the same working conditions. The condition mainly refers to the working temperature and the controlled inlet RH. As for the load profile, as Figure 2 illustrates, we applied the triangle and rectangle load profile to evaluate the developed model. Correspondingly, the cell voltage raised and dropped in a range from 0.4V to 0.9V represented by the yellow line in each subgraph. In Figure 2, the first row explains the forming rate of the oxide coverage. When the cell voltage jumped to the upper level, the forming rate of the oxide coverage gradually increased at first, then exponentially increased until the voltage started to drop. The second, third, and fourth rows explained the kinetic of the platinum dissolution, oxidation, and chemical dissolution. It's obvious that the dissolution affects the catalyst degradation at a level that is more significant than the others under this working condition. The figures in the fifth row present the change rate of the number of particles whose radius is 100nm. It's the mean value of the radius of particles in the initialized PRD. The figures in the sixth row present the evolution of the Pt ion concentration with respect to the load profile. Specifically, we presented the forward and backward reaction rates of the platinum oxidation. According to the right subgraph on the third row, as the cell voltage increased, the forward reaction rate increased rapidly to drive the reaction.

Figure 3 presents the evolution of the membrane thickness in the context of the triangle and the rectangle load profile. Furthermore, in Figure 3 we also present the water transportation through the membrane that includes the mechanism of the diffusion and the electro-osmotic effect. The former is based on the gradient between the water content in the ACL and CCL interface. The water content λ_w of the membrane is described as :

$$\lambda_{\text{mem}} = \begin{cases} 0.043 + 17.81a - 39.85a^2 + 36.0a^3, & \text{if } 0 \leq a \leq 1 \\ 14.0 + 1.4(a-1), & \text{if } 1 < a \leq 3 \end{cases} \tag{30}$$

In this case, we applied a simplified expression of water activity which mathematically equals the RH of the gas :

$$a = \frac{p_{vp}}{p_{vp,sat}} \tag{31}$$

Here the notation "vp" and "sat" denotes the vapor and saturation vapor. The vapor pressure of the anode node and cathode node can be obtained from the solution of the aforementioned macro-scale model. The water transportation from cathode to anode is dominated by load current. A large load current leads to huge water production in the CCL, and consequently raises the water content in the membrane. In contrast, the rate of thickness degradation increased exponentially with respect to the applied potential. According to equation 18, the membrane thickness itself, and the oxygen pressure in the cathode also influence the degradation. As shown in Figure 5, the concentration of oxygen tracked the applied potential closely, as a result of electron consumption from load current.

4. CONCLUSIONS

In this study, a Python-based dual-scale degradation model of PEMFC is developed. The evolution of the stack voltage, membrane thickness and ECSA can be extracted during the long-term simulation to assess the health state of the PEMFC. Benefiting from the proposed model, the Pt catalyst degradation behaviors under various conditions are analyzed with microscopic physical insights. The impact of operating parameters is also revealed explicitly through this analysis.

Nevertheless, the drawback of the developed model still exists. Several aforementioned simplifications of the model may lead to prediction errors that may lead to misjudging from further management strategies. They should be carefully justified. Also, the evolution of the PRD still needs further validation based on experiment data to fix the fitted parameter in the mathematical model.

In future work, we look forward to enhancing our model through experimental validation. On the other hand, based on the physics model, we will seek a suitable model predictive control strategy for health-aware control and energy management systems to improve the durability of a fuel cell system,.

5. ACKNOWLEDGMENTS

This work has been supported by French National Research Agency via project MPC-DEPLOY (Grant no. ANR-23-CE05-0006), ANR ERC Tremplin StG grant (ANR-23-ERCB-0004-01), ANR Chaire de Professeur Junior project (ANR-22-CPJ1-0074-01), and the EIPHI Graduate School (contract ANR-17-EURE-0002) and the Region Bourgogne Franche-Comté

6. REFERENCES

[1] R. Ma et al., « Recent progress and challenges of multi-stack fuel cell systems : Fault detection and reconfiguration, energy management strategies, and applications », Energy Conversion and Management, vol. 285, p. 117015, Jun. 2023

[2] J. Zuo, N. Y. Steiner, Z. Li, and D. Hissel, "Health management review for fuel cells : Focus on action phase," Renewable and Sustainable Energy Reviews, vol. 201, p. 114613, Sep. 2024.

[3] C. Zhang, "A health management review of proton exchange membrane fuel cell for electric vehicles : Failure mechanisms, diagnosis techniques, and mitigation measures," Renewable and Sustainable Energy Reviews, 2023.

[4] P. Gazdzick, J. Mitzel, D. Garcia Sanchez, M. Schulze, and K. A. Friedrich, « Evaluation of reversible and irreversible degradation rates of polymer electrolyte membrane fuel cells tested in automotive conditions », Journal of Power Sources, vol. 327, pp. 86–95, Sep. 2016

[5] H. A. Baroody and E. Kjeang, "Predicting Platinum Dissolution and Performance Degradation under Drive Cycle Operation of Polymer Electrolyte Fuel Cells," Journal of The Electrochemical Society, vol. 168, p. 044524, Apr. 2021

[6] M. Chandesris, R. Vincent, L. Guetaz, J.-S. Roch, D. Thoby, and M. Quinaud, "Membrane degradation in PEM fuel cells : From experimental results to semi-empirical degradation laws," International Journal of Hydrogen Energy, vol. 42, no. 12, pp. 8139–8149, Mar. 2017

[7] W. Touil, Z. Li, R. Outbib, D. Hissel, and S. Jemei, « A System-Level Modeling Framework for Predicting Pt Catalyst Degradation in Proton Exchange Membrane Fuel Cells », 2024, SSRN.

[8] Josef C Meier, Ioannis Katsounaros, Carolina Galeano, et al. "Stability investigations of electrocatalysts on the nanoscale". In : Energy & Environmental Science 5.11 (2012), pp. 9319–9330 (cit. on p. 50).

[9] R. M. Darling and J. P. Meyers, "Kinetic Model of Platinum Dissolution in PEMFCs," J. Electrochem. Soc., vol. 150, no. 11, p. A1523, 2003.

[10] P. Ren, P. Pei, Y. Li, Z. Wu, D. Chen, and S. Huang, "Degradation mechanisms of proton exchange membrane fuel cell under typical automotive operating conditions," Progress in Energy and Combustion Science, vol. 80, p. 100859, Sep. 2020.

[11] J. T. Pukrushpan, "Modeling and control of PEM fuel cell systems and fuel processors".

[12] J. P. Meyers and R. M. Darling, "Model of Carbon Corrosion in PEM Fuel Cells," J. Electrochem. Soc., vol. 153, no. 8, p. A1432, 2006.

[13] W. Touil, Z. Li, R. Outbib, D. Hissel, and S. Jemei, "A system-level modeling framework for predicting Pt catalyst degradation in proton exchange membrane fuel cells," Journal of Power Sources, vol. 625, p. 235628, Jan. 2025